SOVIET PHYSICS JETP VOLUME 26, NUMBER 5 MAY, 1968

KINETICS OF PHYSICAL PROCESSES IN CO_2 *LASERS*

B. F. GORDIETS, N. N. SOBOLEV, and L. A. SHELEPIN

P. N. Lebedev Physics Institute, Academy of Sciences, U.S.S.R.

Submitted June 29, 1967

Zh. Eksp. Teor. Fiz. 53, 1822–1834 (November, 1967)

A method of computing vibrational level populations in CO_2 lasers is proposed. The method postulates the introduction of a vibrational temperature T_i for each vibrational mode. The vibrational and gas temperatures are determined by the equations of the vibrational energy balance and thermal conductivity. Population inversion is computed as function of the relative concentration of CO_2, N_2, and He, total pressure, free electron density, and discharge tube radius. The effect of these parameters on the laser output power is also evaluated. The obtained relationships coincide qualitatively with experimental curves. A quantitative agreement is also present within the limits of accuracy of the investigated model.

1. INTRODUCTION. BASIC COMPUTATION METHOD

At the present time the highest output powers in CW operation (exceeding 1000 W) are obtained from CO_2 lasers, whose efficiency approaches 30%. Therefore a theoretical and experimental investigation of CO_2 lasers a study of the basic physical processes, and an achievement of optimal generation conditions are of considerable significance and are the subject of a large number of studies (see for example the reviews[1,2]).

However we have as yet no coherent picture of the operating mechanism of CO_2 lasers. This is due to the complexity of molecular plasma phenomena and to the multilevel nature of the system, which must be accounted for at the outset in the analysis of relaxation processes.

The analysis of CO_2 lasers should be based on the study of the kinetics of the physical processes. Consequently in the general case it is necessary to solve a set of balance equations for a multilevel system and to find the parameters of plasma of complex chemical composition (CO_2, N_2, He, and other admixtures) as a function of the external conditions. A complete solution of this problem appears unrealistic at this time. Therefore we must make simplified model assumptions.

Figure 1 shows the diagram of vibrational levels of the CO_2 and N_2 molecules. The numbers 1, 2, and 3 denote the levels of symmetric, deformational, and asymmetric vibrations respectively of the CO_2 molecule and 4 denotes the vibrational levels of N_2. A system of rotational sublevels corresponds to each vibrational level. For the sake of simplicity we do not consider the rotational structure of the vibrational level, although in principle it is possible to do so.

A number of problems related to the kinetics of rotational level population were discussed by Witteman[3]. However, the main simplifying assumption consists in the possibility to introduce a vibrational temperature T_i for each vibrational mode in polyatomic molecules (see also[4]). This is due to the fact that the exchange of vibrational quanta within a given mode takes much less time than that taken by the energy transfer to translational degrees of freedom and energy exchange among various modes[5] (for example, in CO_2 lasers the energy pump rate and the rate of relaxation from a given mode at the pressure $P_{CO_2} = 1$ Torr and gas temperature $T = 300^\circ$ amount to $\sim 10^3\ \text{sec}^{-1}$, while the quantum exchange rate in each mode is $\sim 10^6$–$10^7\ \text{sec}^{-1}$). In the general case, these vibrational temperatures differ from one another and from the gas temperature. The ability to introduce a single parameter (vibrational temperature) to characterize the populations of level groups in molecular systems used in lasers simplifies the computation considerably. The system of balance equations for the populations of a large number of levels reduces to a system of a small number of vibrational-energy balance equations for each group of levels. The vibrational temperatures obtained in the course of the solution determine the presence or absence of inverted population at levels belonging to various modes.

This method of computing populations of vibrational levels of polyatomic molecules in the ground state has its limits of applicability, owing to the fact that the exchange of vibrational quanta within each vibrational mode should play the dominant role. Therefore the amount of impurities cannot be much larger than the CO_2 concentration. The second limitation is imposed by the anharmonic nature of the vibrations.

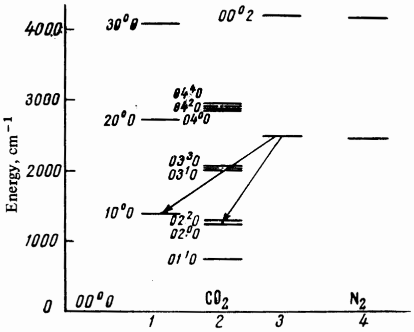

FIG. 1. Vibrational levels of CO_2 and N_2 molecules (laser transitions indicated by arrows).

2. BASIC PHYSICAL PROCESSES: BALANCE EQUATIONS

We now consider the physical processes in CO_2 lasers. We assume that the electrical discharge in the gases $CO_2 - N_2$ and $CO_2 - N_2 - He$ is free of other components (O, CO, N, ON, etc.), i.e., we do not consider dissociation and various chemical reactions in the discharge. This assumption is fully justified in flow-through systems where chemical decomposition of the initial components has not enough time to occur.

Our analysis is based on the following relaxation scheme developed in[4,6]. The electrons excite the vibrational levels of N_2 directly (this process is not considered for the CO_2 molecule). This is followed by a resonant exchange of vibrational energy from N_2 to the 00°v levels of the CO_2 molecule which then undergoes a transition to the deformational mode of vibration through molecular collisions. Further relaxation causes the energy of the deformational vibration mode to change into the energy of translational motion during collisions with the CO_2, N_2, and He molecules. The direct transition from vibrational to translational energy at the 10°0 and 00°1 levels and radiative processes can be neglected[7].

In the stationary case each vibrational mode of CO_2 has its own supply of energy. The quantity of this energy E_i per unit volume for each mode i = 1, 2, 3 of the CO_2 molecules and mode i = 4 of the N_2 molecules is given by

$$E_i = h\nu_i \frac{x_i}{(1-x_i)^2} N_0, \quad E_2 = h\nu_2 \frac{2x_2}{(1-x_2)^3} N_0,$$
$$E_4 = h\nu_4 \frac{x_4}{(1-x_4)^2} N_{04}, \quad i = 1.3; \tag{1}$$

where N_0 and N_{04} are the number of molecules of CO_2 and N_2 respectively per unit volume in ground state; $x_i = \exp(-h\nu_i/kT)$, ν_i are fundamental frequencies of vibration of various modes; and mode i = 2 is twice degenerate.

The following molecular processes are considered in the balance equations for the vibrational energies E_i:

a) $h\nu_4 \to h\nu_3 - \Delta E_{34}$ with probability $W_{34}e^{-\Delta E_{34}/kT}$,
b) $h\nu_3 \to 3h\nu_2 + \Delta E_{32}$ with probability W_{32},
c) $h\nu_3 \to h\nu_1 \to h\nu_2 + \Delta E_{3(1,2)}$ with probability $W_{3(1,2)}$,
d) $h\nu_1 \to 2h\nu_2 + \Delta E_{12}$ with probability W_{12},
e) $h\nu_2 \to$ kinetic energy with probability W_{20}.

Here ΔE_{ik} denotes the corresponding differences of the energies converted into the vibrational (process a) or kinetic (processes b – e) forms. We note that the use of experimental probabilities characterizing the relaxation of the vibrational energies E_i permits us also to account for processes other than the above, such as transitions via higher levels.

From now on we assume that the discharge occurs in a cylindrical tube with radius R and length $L \gg R$. We also assume that electrons and excited CO_2 and N_2 molecules have radial distributions described by the Bessel function of zero order $J_0(2.4r/R)$1). The balance equations for E_1, E_2, E_3, and E_4 in the stationary case then have the form

$$\frac{dE_4}{dt} = h\nu_4 N_{04}\Big\{\alpha_4 W_{e4} N_e + W_{34} N_0 x_3 - \Big(\alpha_4 W_{4e} N_e \times\Big[\int_0^R rJ_0\Big(\frac{r}{\Lambda}\Big)dr\Big]^{-1}\int_0^R rJ_0^2\Big(\frac{r}{\Lambda}\Big)dr + W_{34}e^{-\Delta E_{34}/kT} + \beta_4\frac{D_{N_2}}{\Lambda^2}\Big)x_4\Big\} = 0,$$

$$\frac{dE_3}{dt} = h\nu_3 N_0\Big\{W_{34}e^{-\Delta E_{34}/kT}N_{04}x_4 + W_{3(1,2)}e^{-\Delta E_{3(1,2)}/kT}x_1x_2 + W_{32}e^{-\Delta E_{32}/kT}x_2^3 - \Big(W_{34}N_{04} + \beta_3\frac{D_{CO_2}}{\Lambda^2}N_0 + W_{32} + W_{3(1,2)}\Big)x_3\Big\} = 0,$$

$$\frac{dE_2}{dt} = h\nu_2 N_0\Big\{(3W_{32} + W_{3(1,2)})x_3 + 2W_{12}x_1 - \beta_2\frac{D_{CO_2}}{\Lambda^2}x_2 - W_{3(1,2)}e^{-\Delta E_{3(1,2)}/kT}x_1x_2 - 3W_{32}e^{-\Delta E_{32}/kT}x_2^3 - 2W_{12}e^{-\Delta E_{12}/kT}x_2^2\Big\} - W_{20}[1 - e^{-h\nu_2/kT}][E_2 - E_2^0] = 0, \tag{2}$$

$$\frac{dE_1}{dt} = h\nu_1 N_0\Big\{W_{3(1,2)}x_3 + W_{12}e^{-\Delta E_{12}/kT}x_2^2 - \Big(\beta_1\frac{D_{CO_2}}{\Lambda^2} + W_{12}\Big)x_1\Big\} = 0.$$

Here x_i and the electron density N_e refer to the center of the discharge tube, W_{e4} is the probability (per electron) of exciting N_2 by electron impact, W_{4e} is the probability of the reverse process, α_4 is the average number of vibrational quanta excited by the electrons, D_{N_2} and D_{CO_2} are the coefficients of diffusion of the excited N_2 and CO_2 molecules in the gaseous mixture, $\Lambda = R/2.4$ is the diffusion length, β_i is the average number of vibrational quanta transferred through diffusion; $\beta_i \gtrsim 1$ and depends on the vibrational temperature T_i, and E_2^0 is the energy of deformational vibration corresponding to the gas temperature T.

The system (2) is nonlinear and cumbersome to solve. It is simplified if T_1 and T_2 are small enough and we can neglect the reverse energy transfer into the asymmetric vibrational mode as well as the diffusive decay of the 10°0 level. Assuming that the resonant nature of energy transfer renders the probability W_{34} much larger than all the remaining W_{ik}, we write the solution of (2) in the form

$$x_3 = \alpha_4 W_{e4} N_e N_{04}\Big\{\alpha_4 W_{e4} N_e N_{04}\Big[\int_0^R rJ_0\Big(\frac{r}{\Lambda}\Big)dr\Big]^{-1}\int_0^R rJ_0^2\Big(\frac{r}{\Lambda}\Big)dr + N_0\Big(\beta_2\frac{D_{CO_2}}{\Lambda^2} + W_{32} + W_{3(1,2)}\Big) + \beta_4\frac{D_{N_2}}{\Lambda^2}N_{04}\Big\}^{-1},$$

$$x_2 = \frac{2W_{20}}{2W_{20} + \beta_2 D_{CO_2}/\Lambda^2}x_2^0 + \frac{3(W_{32} + W_{3(1,2)})}{2W_{20} + \beta_2 D_{CO_2}/\Lambda^2}x_3,$$

$$x_1 = \frac{W_{3(1,2)}}{W_{12}}x_3 + \exp\Big(-\frac{\Delta E_{12}}{kT}\Big)x_2^2, \quad x_2^0 = \exp\Big(-\frac{h\nu_2}{kT}\Big). \tag{3}$$

Along with the vibrational temperatures T_i determined by (3) we must consider the gas temperature T. The gas temperature is an important factor that significantly affects the relaxation of vibrational levels, the achievement of population inversion, and generation in molecular lasers[4,8]. This is due to the fact that in the case of molecular lasers operating on vibrational levels the lower working level lies relatively close to the ground state and its population is largely determined by the gas temperature; furthermore, the probabilities involved in molecular collisions strongly depend on T. We must therefore add the thermal conductivity equation that determines the gas temperature in the stationary case to system (2). (Heat flow by con-

---

1) This assumption is valid if the loss of electrons and excited molecules occurs only at the tube walls due to diffusion. In the investigated cases this condition is always true for the electrons, but not for excited molecules at pressures $p \gtrsim 1$ Torr. In practice, however, this does not affect the results of computation. We note that since the true distribution is unknown, the choice of the Bessel distribution is preferable by virtue of the simplicity of the expression $D_i\,\Lambda^2$ for the diffusive decay probability.

$$\lambda_{mix}=\frac{\lambda_{CO_2}}{1+0{,}81p_{N_2}/p_{CO_2}+0{,}23p_{He}/p_{CO_2}}+$$
$$+\frac{\lambda_{N_2}}{1+1{,}4p_{CO_2}/p_{N_2}+0{,}34p_{He}/p_{N_2}}+\frac{\lambda_{He}}{1+3{,}4p_{CO_2}/p_{He}+2{,}7p_{N_2}/p_{He}}. \quad (6)$$

The magnitudes and thermal dependencies of the coefficients of thermal conductivity for pure gases λCO_2, λN_2, and λHe were taken from[16].

4. COMPUTATION RESULTS

The system of equations (2) was solved together with (4) to determine the conditions governing the population inversion of the 00°1 and 10°0 levels of the CO_2 molecule and its behavior in response to changes of various parameters (composition of the mixture, total pressure, and electron density). The solution was obtained with the aid of (3). The computation was based on the following values: kT_e = const = 3 eV, $\alpha_4 = 3.5$, $\beta_4 = \beta_3 = 1.5$, $\beta_2 = 1$, and R = 12.5 mm. The results are given in Figs. 3–10.

Figure 3 shows population inversion as a function of nitrogen pressure. At first, as we add nitrogen, the energy pumped into the asymmetric vibration mode increases and the population inversion increases. However, further addition of N_2 causes the gas temperature to rise, resulting in an increasing relaxation rate and reduced population of the 00°1 level. The rising temperature is also accompanied by increasing population of the lower laser level 10°0. These factors combine to produce a pressure $pN_2 \sim 1$–2 Torr characterizing the maximum inversion. We note here that consideration of the effect of N_2 on the relaxation of the 00°1 level should shift the optimum somewhat towards lower values of nitrogen pressure and should result in a steeper drop of population inversion with increasing concentration of N_2.

Figure 4 shows population inversion as a function of CO_2 pressure. The optimum CO_2 pressure (~1–2 Torr) here is due to the competition of two factors: an increased number of CO_2 molecules on the one hand, and an increased decay rate of the 00°1 level due to increased gas temperature and CO_2 pressure on the other.

The effect of helium on the population inversion is illustrated by Fig. 5, representing the latter as a function of helium pressure. Since the thermal conductivity of helium is several times greater than that of CO_2 and N_2, it decreases the gas temperature and thus enhances the population inversion. A consideration of the effect of helium on the relaxation rate of the 00°1 level should reveal an optimum helium pressure accompanying the maximum inversion.

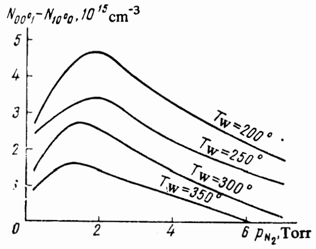

FIG. 3. Population inversion as a function of nitrogen pressure for the mixture 2 Torr Co$_2$ + x Torr N_2 ($\bar{N}_e = 7.5 \times 10^9$ cm^{-3}) at various temperatures of the tube wall.

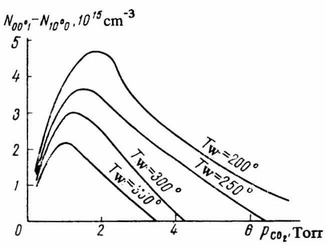

FIG. 4. Population inversion as a function of CO_2 pressure for the mixture 2 Torr N_2 + x Torr CO_2 ($\bar{N}_e = 7.5 \times 10^9$ cm^{-3}) at various temperatures of the tube wall.

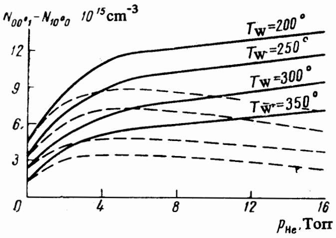

FIG. 5. Population inversion as a function of helium pressure for the mixture 2 Torr CO_2 + 2 Torr N_2 + x Torr He ($\bar{N}_e = 7.5 \times 10^9$ cm^{-3}) at various temperatures of the tube wall (dashed lines denote a rough estimate of the effect of helium on the relaxation rate of the 00°1 level).

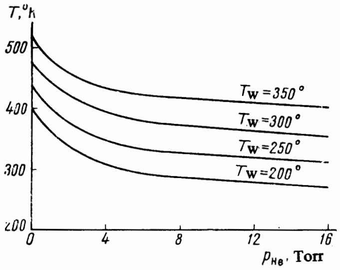

FIG. 6. Gas temperature as a function of helium pressure for the mixture 2 Torr CO_2 + 2 Torr N_2 + x Torr He ($N_e = 7.5 \times 10^9$ cm^{-9}) at various temperatures of the tube wall.

Figure 6 shows the variation of gas temperature with the addition of helium. The behavior of the pressure-dependence of temperature agrees with the experimental data[8].

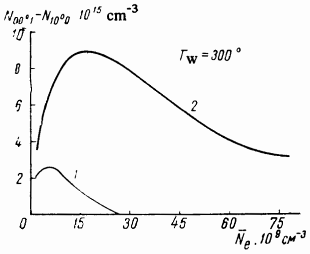

FIG. 7. Population inversion as a function of electron density for the mixtures 2 Torr CO_2 + 2 Torr N_2 (line 1) and 2 Torr CO_2 + 2 Torr N_2 + 6 Torr He (line 2).

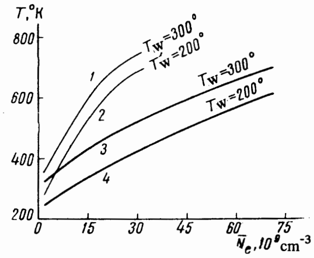

FIG. 8. Gas temperature as a function of electron density for the mixtures 2 Torr CO_2 + 2 Torr N_2 (lines 1 and 2) and 2 Torr CO_2 + 2 Torr N_2 + 6 Torr He (lines 3 and 4) at various temperatures of the tube wall.

Population inversion and gas temperature are shown in Figs. 7 and 8 as functions of mean electron density $\bar{N}_e$. The two competing factors, increasing pumping to the upper laser level and increased temperature result in optimum values of electron densities. The shift of the optimal values of $\bar{N}_e$ toward the high side in the presence of helium in the discharge is typical here. This is due to the fact that the drop in temperature caused by the addition of helium permits us to enhance the energy transfer to the asymmetric vibrational mode of CO_2 increasing $\bar{N}_e$ and thus causing population inversion to increase. Such a shift of the optimum was observed experimentally[18].

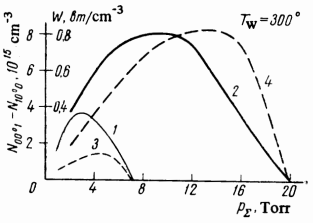

FIG. 9. Population inversion (solid lines 1 and 2) and output powers (dashed lines 3 and 4) as functions of total pressure p_Σ for the mixtures $CO_2:N_2 = 1:1$, $\bar{N}_e = 7.5 \times 10^9$ cm⁻³ (lines 1 and 3) and $CO_2:N_2:He = 1:1:3$, $\bar{N}_e = 3 \times 10^{10}$ cm⁻³ (lines 3 and 4).

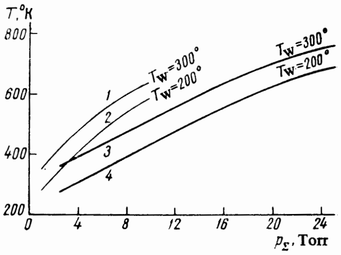

FIG. 10. Gas temperature as a function of total pressure p_Σ for the mixtures $CO_2:N_2 = 1:1$, $\bar{N}_e = 7.5 \times 10^9$ cm⁻³ (lines 1 and 2) and $CO_2:N_2:He = 1:1:3$, $\bar{N}_e = 3 \times 10^{10}$ cm⁻³ (lines 3 and 4) for various temperatures of the tube wall.

Figures 9 and 10 show the dependence of population inversion (solid lines) and gas temperature respectively on total pressure p_Σ with the relative concentration of the mixture components held constant. The presence of the optima in the pressure functions is due to the same factors as above.

Since according to our computations and experimental data[12] $\bar{N}_e$ weakly depends on gas pressure at a constant discharge current, the functions of $\bar{N}_e$ and pressure (with constant $\bar{N}_e$) obtained here can be compared with the ordinary experimental functions of current and pressure (with constant current). Given the above pressures and tube radius, we can assume that $\bar{N}_e = 7.5 \times 10^9$ cm^{-3} corresponds to a current of ~20 mA and is proportional to the current. The behavior of inversion and gas temperature as functions of total pressure and $\bar{N}_e$ (current) is in good agreement with experimental data[8,18,19]. The computed optimal values of pressures and $\bar{N}_e$ (currents) are also typical in experimental practice.

The effect of the discharge tube radius on the population inversion is illustrated by Fig. 11, which shows population inversion as a function of CO_2 pressure at various tube radii. The computations were performed with constant $\bar{N}_eR^2 = 1.17 \times 10^{10}$ cm^{-1} (corresponding to a direct discharge current of ~20 ma). We see that the maximum obtainable inversion and the corresponding optimum pressure of CO_2 increase with decreasing radius. This is due to the fact that gas temperature hardly varies at constant $\bar{N}_eR^2$, yet a tube with smaller radius has a higher electron density ($\bar{N}_e \sim 1/R^2$) and consequently a larger energy transfer (per unit volume) to the asymmetric vibrational mode of CO_2. Such a dependence of population inversion on tube radius was obtained experimentally (in a sealed system)[19] and the relationship between the radius and optimal CO_2 pressure ($p^{\text{opt}}_{CO_2} \cdot 2R \approx 4$ Torr·cm) as determined there by experiment is close to the theoretical value (≈3.3 Torr·cm). Inversion increases with decreasing tube radius also when $\bar{N}_e$ (current density) is held constant. The cause of this is the lower gas temperature in a thinner tube (see (4)) at constant pump rate ($\bar{N}_e$ = const).

Along with the above dependencies of population inversion on various parameters, we can also propose a qualitative explanation of other experimental results. For example, the radial gain profiles obtained in[19] in various mixtures and their departure from the Bessel distribution are fully attributable to the volume decay of vibrationally excited CO_2 molecules and a change in the relaxation rate of the upper laser level when the composition, pressure, and temperature of the mixture are varied. The increase of population inversion along the tube axis observed experimentally when helium is added to the discharge is due to the fact that the resulting noticeable drop in gas temperature occurs at the axis.

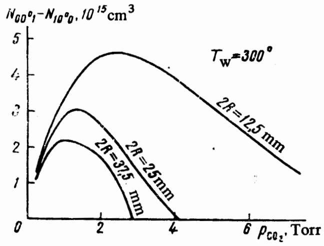

FIG. 11. Population inversion as a function of CO_2 pressure for the mixture 2 Torr N_2 + x Torr CO_2 at various radii R of the discharge tube ($\bar{N}_eR^2 = 1.17 \times 10^{10}$ cm⁻¹).

As we noted above, along with the good qualitative agreement of our analysis with the experimental data there is also a good quantitative agreement for a number of parameters (computed values of optimum pressures and electron concentrations, and the shift of these optima occurring with the addition of helium). Nevertheless the computed absolute values of population inversion differ by a factor of 5–7 from the data of Statz, Tang, and Koster[7]. It seems that this difference cannot be eliminated by rendering their results more precise. We think that this is due in the first place to the possible effect of electron excitation on the population of the lower laser level (electron excitation of the deformational and symmetric vibration modes) and then to the effect of N_2 and He on the decay of the upper level. Therefore a sufficiently accurate computation and experimental determination of the indicated cross sections constitute a fairly urgent problem. The experimental study of the radial distribution of gas temperature, particle density, and the electron distribution function can be very useful in making the above analysis more precise.

5. GENERATION REGIME. CONCLUSION

The majority of experimental work with CO_2 lasers consists in the investigation of the operating characteristics of the generator. However a fairly complete theoretical solution of this problem is quite difficult since we must know the distribution of the radiation field within the resonator, consider the rotational relaxation and the competition of vibrational-rotational transitions, and take the effect of various modes into account. For a qualitative explanation of the parametric dependence of the output power we use a simplified model of relaxation in the generating plasma. Here the terms

$$-h\nu_3 B_{31} E^2 \int_0^R 2\pi r J_0\left(\frac{r}{\Lambda}\right)\varphi(r)\,dr\,(n_3^J - n_1^{J+1})$$

and

$$+h\nu_1 B_{31} E^2 \int_0^R 2\pi r J_0\left(\frac{r}{\Lambda}\right)\varphi(r)\,dr\,(n_3^J - n_1^{J+1}),$$

vection can be neglected according to Vasil'ev and Sergeenkova[9].) The simplified equation of thermal conductivity yields a simple relation that can be used to find a mean gas temperature T[9]:

$$Q(T) = (T - T_w)\,18.9\,\lambda_{mix}(T).$$

Here Q(T) is the energy liberated in the gas in unit time per unit of discharge length, T_W is the temperature of the discharge tube wall, and $\lambda_{mix}(T)$ is the coefficient of thermal conductivity of the gas mixture.

We further assume that Q(T) is determined by the energy that is converted by relaxation from vibrational to translational degrees of freedom[10][2]. In the stationary case the energy pumped into vibrational degrees of freedom of CO_2 and N_2 (and after relaxation into translational degrees of freedom) can be determined as follows

$$Q(T) = 2\pi a_4 h\nu_4 N_e N_{04}\left[W_{e4}\int_0^R rJ_0\left(\frac{r}{\Lambda}\right)dr - x_4(T)\,W_{4e}\int_0^R rJ_0^2\left(\frac{r}{\Lambda}\right)dr\right].$$

Here the first term represents a flow of energy from the electrons to the vibrational degree of freedom of N_2, while the second term defines the reverse flow. Consequently to determine the gas temperature we obtain the equation

$$Q(T) = 1{,}36R^2 a_4 h\nu_4 N_e N_{04}[W_{e4} - 0.63W_{4e}x_4(T)] = (T - T_w)\cdot 18.9\lambda_{mix}(T \tag{4}$$

Together with (2) this equation determines the vibrational temperatures T_i and the gas temperatures T for given partial pressures of the gas mixture, and the density and mean energy of the electrons.

3. GAS DISCHARGE PARAMETERS: PROCESS PROBABILITIES.

To solve (2) together with (4) we must properly select the probabilities of the processes and plasma parameters.

To find the probabilties of electron excitation of the vibrational levels of nitrogen we must know the excitation cross section, electron density N_e, the average electron energy, and the shape of the distribution function. The total excitation cross section σ of the first eight vibrational levels of nitrogen was found by Chen and Schulz[11]. According to our theoretical computations and experiment[12] the average electron energy in a typical discharge used in CO_2 lasers lies within the region corresponding to the large excitation cross section of N_2 vibrational levels (2–4 eV). We can therefore expect that the shape of the distribution function has no great effect on the vibrational excitation probability. A Maxwellian distribution is assumed from now on.

Figure 2 shows $W_{e4} = \langle \sigma v \rangle$ (v is electron velocity averaged with respect to Maxwellian distribution) as a function of electron temperature T_e. When $kT_e \gtrsim 2$ eV we see that the vibrational excitation probability depends on the temperature rather weakly.

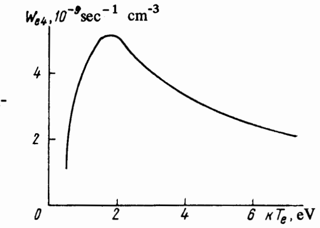

FIG. 2. Probability of electron excitation of a group of vibrational N_2 levels (per electron).

An exact computation of electron temperature and density is practically not possible. Starting with von Engel's theory of the positive column (whose applicability is limited, of course) we carried out a semi-empirical computation of N_e and T_e in the gas mixture as a function of the partial pressures. In doing this we used the experimental data for the electric discharge in pure gases given in[13]. The computed T_e differed from the experimental value[12] by not more than a factor of two and the computed N_e differed by not more than a factor of four. A comparison of experimental and theoretical values furnished the basis for selecting N_e and T_e for the analysis.

Molecular collision probabilities are not sufficiently known. Various experiments and theoretical computations frequently give results that differ by a factor of several units. The table shows the most reliable probabilities in our view, at three temperatures (taking into account the variation of the number of molecular collisions with temperature) selected according to[14]. The probabilities are given in reciprocal seconds at a pressure of 1 Torr (at 300°K). For the remaining temperature values within the range 300–1000°K the probabilities were obtained by interpolating the given values.

T°, K	W_{20} CO_2–CO_2	W_{20} CO_2–N_2	W_{20} CO_2–He	W_{12} CO_2–CO_2	W_{32} CO_2–CO_2	$W_{3(1,2)}$ CO_2–CO_2
300	$2{,}1\cdot10^2$	$6{,}6\cdot10^2$	$6{,}5\cdot10^3$	$1{,}8\cdot10^4$	$7\cdot10^1$	$1{,}4\cdot10^2$
600	$3{,}3\cdot10^3$	10^3	$6{,}5\cdot10^3$	$5{,}3\cdot10^4$	$8\cdot10^2$	$1{,}2\cdot10^3$
1000	$2{,}4\cdot10^4$	$1{,}3\cdot10^3$	$6{,}5\cdot10^3$	$1{,}8\cdot10^5$	$5\cdot10^3$	$8\cdot10^3$

With a tube diameter of 2R ~ 25 mm and gas mixture pressures $p_\Sigma \lesssim 3$ Torr, vibration-excited molecules are lost mainly by diffusion towards the tube walls. Assuming that the concentration of the excited molecules is low, the coefficients of diffusion D_{N_2} and D_{CO_2} in the gas mixture are determined by the following formulas[15] for given partial pressures p_i of the mixture components:

$$\frac{1}{D_{N_2}} = \frac{p_{N_2}}{D_{N_2-N_2}} + \frac{p_{CO_2}}{D_{N_2-CO_2}} + \frac{p_{He}}{D_{N_2-He}}, \tag{5}$$

$$\frac{1}{D_{CO_2}} = \frac{p_{CO_2}}{D_{CO_2-CO_2}} + \frac{p_{N_2}}{D_{CO_2-N_2}} + \frac{p_{He}}{D_{CO_2-He}}$$

The computation was based on the following coefficients of self-diffusion and diffusion in binary mixtures at 300°K and pressure of 1 Torr[16]: $D_{N_2-N_2}$ = 160 cm²/sec, $D_{CO_2-CO_2}$ = 86 cm²/sec, $D_{N_2-CO_2}$ = 130 cm²/sec, D_{N_2-He} = 560 cm²/sec, and D_{CO_2-He} = 500 cm²/sec; the temperature dependence was assumed to be $\sim T^{2/3}$. The coefficient of thermal conductivity of the gas mixture λ_{mix} was computed from[17]:

---

[2] Simple computation shows that elastic collisions between electrons and molecules at these densities cannot account for any noticeable heating of gas observed experimentally [8]. We also neglect other processes (ion current to the walls, dissociation, etc.). in the energy balance. The high efficiency of CO_2 lasers and the satisfactory agreement between the theoretical results (see below) and experimental data confirm the validity of this assumption.

are added to the second and fourth equations of (2) respectively. The added terms describe the relaxation of the energy of the asymmetric and symmetric vibrational modes of the CO_2 molecule in response to the radiation field.

Here B_{31} is the Einstein coefficient of stimulated emission, E is the radiation field amplitude in the center of the discharge tube, $n_3^J - n_1^{J+1}$ is the vibrational-rotational population inversion of the working levels in the center of the tube, J is the rotational quantum number, and $\varphi(r)$ is the radial distribution of the squared radiation field (from now on assumed to be Besselian). For the sake of simplicity we assume that generation occurs only in a single vibrational-rotational transition $00^\circ 1$ (J = 21) → $10^\circ 0$ (J = 22).

To determine E, the obtained system describing the relaxation of vibrational energy should be completed by adding one more equation[20]. This equation expresses the relationship between the vibrational-rotational inversion $n_3^J - n_1^{J+1}$ in the generating regime with resonator parameters[3]:

$$n_3{}^J - n_1{}^{J+1} = \frac{8\pi \nu_{31}{}^2 R}{0{,}62 \cdot 2c^2 \cdot 2(\pi \ln 2)^{1/2} \pi \Delta\nu_{31} L A_{31}}. \tag{7}$$

Here ν_{31} is the frequency of the working transition, $\Delta\nu_{31}$ is the line width (Doppler contour), c is the velocity of light, L is the length of the resonator, R is the effective coefficient of reflection, and A_{31} is the probability of spontaneous transition; we also took into account the fact that $\varphi(r) = J_0(r/\Lambda)$.

We now turn from the rotational to the vibrational population inversion assuming that the rotational sublevels of vibrational levels have a Boltzman population with gas temperature[7]:

$$\begin{aligned} N_0(x_3 - x_1) &= N_{00^\circ 1} - N_{10^\circ 0} = \\ &= \frac{kT}{2hcB}(2J+1)^{-1} \exp\left\{\frac{hcB}{kT} J(J+1)\right\} (n_3{}^J - n_1{}^{J+1}), \end{aligned} \tag{8}$$

where B is the rotational constant. The cumbersome analytical solution with respect to x_i and E of (2) corrected for the generating regime is considerably simplified in conjunction with (7) and (8) if we assume that the gas temperature and the population of the lower laser level remain the same as before generation[3)].

Based on the above assumptions we computed the output power of the generator with L ≈ 200 cm and R ≈ 0.5 per cubic centimeter (at the tube axis) as a function of total pressure (Fig. 9, dotted lines). A similar computation was performed to determine output power as a function of electron density (current) and partial pressure of CO_2. This procedure also yielded the $\bar{N}_e$ and pressure values corresponding to the maximum power. The presence of optimal pressures and electron densities is due to the same factors as those operating before generation. The optimum pressures agree with the experimental data. The graph shows that there is a shift of the optimum pressure towards the high side and a steeper drop of power with increasing p_Σ as compared to the optimum values and the behavior of population inversion prior to generation.

The relationships presented in Figs. 3–6 and computed at various tube wall temperatures show that external cooling has a substantial effect on population inversion and output power in agreement with experimental data (see for example[1,19]). It is of interest to note that if during generation the electric energy supplied to the discharge remains the same as prior to generation, the gas temperature is lower during generation because a noticeable portion of the energy escapes as radiation due to the high efficiency. For an efficiency of ~25%, the temperature drop is estimated at 8%. We note that the absolute values of computed power are found to be several times higher than the experimental values. This is quite understandable in view of the approximate nature of the computation and the indeterminacy of the process probabilities. Nevertheless the maximum computed increase in output power resulting from the addition of helium is the same as in the experiment (~6 times)[3].

The computations show that, other factors being equal, the lowest possible gas temperature is necessary to improve laser operation. Together with the use of admixtures and good internal cooling, gas temperature can be decreased by the introduction of auxiliary surfaces within the discharge tube. Another possible method of improving laser operation is proper selection of the cross sectional configuration of the tube. However since this can affect the discharge conditions the final conclusion is possible only after suitable experimentation.

The methodology discussed in this paper thus permits us to compute energy level populations and plasma parameters in the CO_2 laser. In spite of the simplicity of the proposed model the results obtained correctly reflect the qualitative nature of experimental relationships: we also observe a quantitative agreement with experiment and the approach towards optimal generation conditions. A number of factors that we failed to take into account (electron excitation of CO_2, population of rotational levels, and the effect of impurities on the relaxation rate of the upper working level) can be readily included in the analysis although some difficulties connected with the computation of the corresponding cross sections remain. As for the generation regime, further approximation of the model is necessary for the quantitative computation.

The authors are indebted to A. I. Osipov and V. V. Sokovikov for discussions.

[3)] This assumption is valid if the generation regime has an auxiliary mechanism to clear the lower working level. This role can be assumed by water vapor added to the working gas mixture [3].

[1] N. N. Sobolev and V. V. Sokovikov, Usp. Fiz. Nauk 91, 425 (1967) [Sov. Phys.-Usp. 10, 153 (1967)].

[2] V. P. Tychinskiĭ, Usp. Fiz. Nauk 91, 389 (1967) [Sov. Phys.-Usp. 10, 131 (1967)].

[3] W. J. Witteman, Philips Research Rep. 21, 73 (1966). J. Quantum Electronics **QE**-2, 375 (1966).

[4] B. F. Gordiets, N. N. Sobolev, V. V. Sokovikov, and L. A. Shelepin, Phys. Lett. **25A**, 173 (1967).

[5] E. V. Stupochenko, S. A. Losev, and A. I. Osipov, Relaksatsionnye protsessy v udarnykh volnakh (Relaxation Processes in Shock Waves), Nauka, 1965.

[6] N. N. Sobolev, and V. V. Sokovikov, ZhETF Pis.

Red. **4**, 303 (1966) and **5**, 122 (1967) [JETP Lett. **4**, 204 (1966) and **5**, 99 (1967)].

[7] H. Statz, C. L. Tang, and J. F. Koster, J. Appl. Phys. **37**, 4278 (1966).

[8] A. I. Sviridov, N. N. Sobolev, and G. G. Tselikov, ZhETF Pis. Red. **6**, 542 (1967) [JETP Lett. **6**, 62 (1967)].

[9] S. S. Vasil'ev and E. A. Sergeenkova, ZhFKh **40**, 2373 (1966).

[10] L. M. Biberman and A. Kh. Mnatsakanyan, Teplofizika vysokikh temperatur **1**, 491 (1966).

[11] G. J. Schulz, Phys. Rev. **A135**, 988 (1964), J. C. Y. Chen, J. Chem. Phys. **41**, 3263 (1964).

[12] P. O. Clark and M. R. Smith, Appl. Phys. Lett. **9**, 367 (1966).

[13] S. C. Brown, Introduction to Electrical Discharges in Gases, Wiley.

[14] T. L. Cottrell and J. C. McCubrey, Molecular Energy Transfer in Gases, London, Butterworths, 1961. G. Lambert, in: Atomic and Molecular Processes, D. Bates, ed. Academic Press, 1962. K. F. Herzfeld, Disc. Faraday Soc. **33**, 22 (1965). P. V. Slobodskaya, Opt. Spektrosk. **22**, 29 (1967).

[15] A. Dalgarno, in: Atomic and Molecular Processes, D. R. Bates, ed. Academic Press, 1962.

[16] G. Hirschfelder, C. Curtiss, and R. Byrd, Molecular Theory of Gases and Liquids, Wiley, 1964.

[17] S. Mathur and S. C. Saxena, Appl. Sci. Res. **17**, 155 (1967).

[18] E. T. Antropov, I. A. Silin-Bekchurin, and N. N. Sobolev, Phys. Lett. in press.

[19] P. K. Cheo and H. G. Cooper, J. Quan. Electronics **QE-3**, 2, 73 (1967).

[20] E. M. Belenov and A. N. Oraevskiĭ, Opt. Spektrosk. 18, 858 (1965).

Translated by S. Kassel
209